Title

Estimates of brain age for gray matter and white matter in younger and older adults: Insights into human intelligence

Authors

Shokri-Kojori, Ehsan
Bennett, Ilana J
Tomeldan, Zuri A
et al.

Publication Date

2021-07-01

DOI

10.1016/j.brainres.2021.147431

Peer reviewed

Brain Research 1763 (2021) 147431

Contents lists available at ScienceDirect

Brain Research

journal homepage: www.elsevier.com/locate/brainres

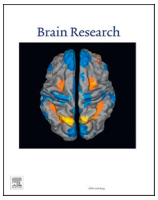

Estimates of brain age for gray matter and white matter in younger and older adults: Insights into human intelligence

Ehsan Shokri-Kojori [a,*], Ilana J. Bennett [a,b], Zuri A. Tomeldan [a], Daniel C. Krawczyk [a,c], Bart Rypma [a,c]

[a] Center for BrainHealth®, School of Behavioral and Brain Sciences, The University of Texas at Dallas, Dallas, TX, USA
[b] Department of Psychology, University of California, Riverside, Riverside, CA, USA
[c] Department of Psychiatry, The University of Texas Southwestern Medical Center at Dallas, Dallas, TX, USA

ARTICLE INFO

Keywords:
Diffusion tensor imaging (DTI)
Fluid intelligence
Crystalized intelligence
Gray matter
White matter
Brain age

ABSTRACT

Aging entails a multifaceted complex of changes in macro- and micro-structural properties of human brain gray matter (GM) and white matter (WM) tissues, as well as in intellectual abilities. To better capture tissue-specific brain aging, we combined volume and distribution properties of diffusivity indices to derive subject-specific age scores for each tissue. We compared age-related variance between WM and GM age scores in younger and older adults and tested whether tissue-specific age scores could explain different effects of aging on fluid (G*f*) and crystalized (Gc) intelligence in younger and older adults. Chronological age was strongly associated with GM ($R^2 = 0.73$) and WM ($R^2 = 0.57$) age scores. The GM age score accounted for significantly more variance in chronological age in younger relative to older adults ($p < 0.001$), whereas the WM age score accounted for significantly more variance in chronological age in older compared to younger adults ($p < 0.025$). Consistent with existing literature, younger adults outperformed older adults in G*f* while older adults outperformed younger adults in Gc. The GM age score was negatively associated with G*f* in younger adults ($p < 0.02$), whereas the WM age score was negatively associated with Gc in older adults ($p < 0.02$). Our results provide evidence for differences in the effects of age on GM and WM in younger versus older adults that may contribute to age-related differences in G*f* and Gc.

1. Introduction

The brain is comprised of gray matter (GM: hosting neuronal cell bodies) and white matter (WM: hosting axonal connections) that are differentially affected by aging (Kochunov et al., 2007; Levakov et al., 2020). For both tissue types, aging is associated with reductions in volume (Ge et al., 2002b; Madan and Kensinger, 2018) and alterations in macromolecule density (Ge et al., 2002a) and microstructure (Benedetti et al., 2006; Bennett et al., 2010; Bennett and Rypma, 2013). GM volume often shows a monotonic decline across the adult lifespan, whereas WM volume decreases only after age 40 (Ge et al., 2002b; Sowell et al., 2003). Diffusion tensor imaging (DTI) studies have revealed decreases in measures that capture the degree of restricted diffusion (i.e., fractional anisotropy, FA) across the adult lifespan in WM (Kennedy and Raz, 2009; Michielse et al., 2010), but increases in FA in deep brain GM structures (Pfefferbaum et al., 2010). Other DTI measures of microstructural properties such as axial diffusivity (AD) and radial diffusivity (RD) are also differentially sensitive to the effects of age on WM and GM structures (Pfefferbaum et al., 2010; Sexton et al., 2014). Prior work has investigated the associations between GM properties (e.g., volume, myelination, and diffusivity) with WM microstructure across the life span (Grydeland et al., 2013; Kochunov et al., 2011; Nazeri et al., 2015), yet less attention has been paid to means for assessing age-related differences between GM and WM when volume and tissue-wide distribution of microstructural measures are considered at the same time.

A handful of studies have assessed the effects of aging on GM and WM tissues in the same cohort (Chiapponi et al., 2013; Farokhian et al., 2017) which may have implication for age-related differences in behavior (Anatürk et al., 2018). GM and WM volume have been associated with the magnitude of diffusivity in WM (e.g., AD and RD) across the adult life span though they had weaker associations with WM anisotropy (Pareek et al., 2018; Rathee et al., 2016). These effects may

* Corresponding author. Present address: Laboratory of Neuroimaging, National Institute on Alcohol Abuse and Alcoholism, National Institutes of Health, Bethesda, MD, USA.
E-mail address: ehsan.shokrikojori@nih.gov (E. Shokri-Kojori).

https://doi.org/10.1016/j.brainres.2021.147431
Received 27 May 2020; Received in revised form 1 February 2021; Accepted 10 March 2021
Available online 15 March 2021
0006-8993/Published by Elsevier B.V.

highlight differences in processes that contribute to age-related differences in volumetric and diffusivity indices. Thus, a more complete understanding of GM and WM aging calls for approaches that combine age-related effects on both macro-structural (volume) and micro-structural (diffusivity) properties in each tissue type, while enabling a direct comparison between age-related differences in WM and GM. Here we used a combined set of volumetric and diffusivity measures to study differences in the effects of age on GM and WM tissues in younger versus older adults.

Whole-brain distribution of diffusivity measures are useful for characterizing global effects of aging on the brain while voxel-wise or ROI analyses offer an opportunity to localize the effect of aging on brain tissues. Considering the heterogeneity of aging effects across brain regions and across individuals (Raz et al., 2005), we studied whole-brain volumetric and microstructural measures of GM and WM across participants (Benedetti et al., 2006; Bennett et al., 2010; Ge et al., 2002b; Salminen et al., 2016) that reflected contributions from all tissue subregions while not being constrained by selection of individual regions within GM and WM. Because of the non-Gaussian distribution of diffusivity measures, whole-brain mean measures may be insufficient to capture the shape of distributions (Charlton et al., 2006). In this respect, differences in higher moments of whole-brain distribution of diffusivity measures, such as increased FA skewness in WM, have been effective in characterizing relevant neurological disorders (Benson et al., 2007; de la Plata et al., 2011; Della Nave et al., 2007). In the present study we used mean, variance, and skewness of brain-wide distribution properties of GM and WM (Charlton et al., 2010; Müller et al., 2006) for FA, AD, and RD indices to estimate effects of age on GM and WM.

Variations in intellectual abilities across the adult lifespan have been observed since the inception of psychometric assessment (Foster and Taylor, 1920). At the population level, aging has been associated with monotonic declines in novel problem-solving and reasoning abilities (fluid intelligence, *Gf*), and stability or improvement in general world knowledge and vocabulary (crystalized intelligence, *Gc*) (Salthouse, 2004). In addition, structural properties of GM and WM have been associated with individual differences in intelligence (Chen et al., 2020; Nestor et al., 2015). These results suggest potential differences in the neurobiological substrates that contribute to the effects of aging on fluid and crystalized abilities (Colom et al., 2009; de Mooij et al., 2018; Góngora et al., 2020; Ohtani et al., 2017; Penke et al., 2012; Wickett et al., 2000), which may be related to different effects of aging on GM and WM. Thus, as a secondary aim, we explored tissue specific contributions to age-related individual differences in *Gf* and *Gc* (Colom et al., 2010).

Here we provide a novel assessment of aging of brain tissues by examining the degree to which a combination of volume and distribution properties of diffusivity measures of WM and GM predicted chronological age in younger and older adults. Previous research has highlighted differences in myelination growth and degenerative processes before and after age 40 (Ge et al., 2002b; Sowell et al., 2003), suggesting non-identical age effects on GM and WM (Abe et al., 2008; Bender et al., 2016; Pfefferbaum and Sullivan, 2015; Raz et al., 2005). Thus, we hypothesized that WM and GM are differently affected by aging in younger versus older adults and that these differences may contribute to age-related differences in *Gf* and *Gc* (Cole et al., 2017a). We computed the age score of WM and age score of GM and compared the extent to which they are associated with chronological age in younger versus older adults ($n = 97$). We explored the degree to which estimates of GM and WM age scores predicted *Gf* and *Gc* abilities in a subgroup of younger ($n = 20$) and older ($n = 19$) participants, and assessed the specificity of the associations with *Gf* and *Gc* to sub-regions of WM and GM.

2. Results

2.1. GM and WM age scores

We calculated subject-specific estimates of volume and distribution properties (mean, variance, and skewness) of FA, AD, and RD, separately for whole-brain WM (Fig. 1A–C) and whole-brain GM (Fig. 1D–F) in 97 adults (age: $M = 43.74$, $SD = 19.65$). For GM, a stepwise regression of chronological age on the 10 volumetric and diffusivity predictors (see Methods) resulted in the selection of volume, FA (variance), AD (mean, skewness), and RD (mean, variance) as significant predictors of chronological age. For WM, a stepwise regression of chronological age on the 10 volumetric and diffusivity predictors resulted in the selection of FA (skewness), AD (mean), and RD (variance) as significant predictors of chronological age. For each participant, GM and WM age scores were calculated using regression coefficients obtained for the tissue-specific predictors while omitting the participant from the model (Fig. 1G, see Methods). Between iterations of omitting each participant, the maximum coefficient of variation for the GM parameters estimates was 5.3% whereas for WM it was 2.7%. The GM age score accounted for 73% of chronological age variance, whereas the WM age score accounted for 57% of chronological age variance across the adult lifespan (Fig. 2A, B). For GM, the standard deviation of the difference between the age score and chronological age was 10.1 years whereas for WM it was 12.9 years. Replacing the stepwise regression with a lasso regression for variable selection resulted in almost identical age scores (see Methods and Supplementary Results and Supplementary Fig. 1).

A notable difference between the tissue-specific age scores was the inclusion of volume for predicting the GM age score but not for predicting the WM age score. We directly tested the contribution of volume only to the effects of age on WM and GM. We found that the GM age score obtained by using volume as the only predictor explained 31% of the variance in chronological age, whereas the WM age score obtained based on volume as the only predictor, explained 5% of the variance in chronological age. Inclusion of diffusivity-related regressors for estimating the GM age score accounted for significantly higher proportions of variance in chronological age than when only GM volume was used as a predictor ($R^2 = 0.73$ vs. $R^2 = 0.31$, $F(5, 90) = 28.29$, $p < 0.0001$). This observation suggested that distribution properties of diffusivity indices of GM are sensitive to aspects of aging that are not captured by conventional volumetric measures. By contrast, distribution properties of diffusivity indices captured most of age-related differences in WM. The data suggest that distribution properties of diffusivity measures are significant predictors of age-related differences in both GM and WM.

2.2. GM and WM age in younger and older adults

For GM and WM, we separately assessed age-related differences in younger and older adults. The patterns of age-related differences in the adult life span suggested that WM and GM may differ in the extent to which they are affected by aging in younger versus older adults (Fig. 2A, B). To assess this more directly, we defined younger and older age groups with a threshold of 40 years of age (Ge et al., 2002a; Sowell et al., 2003) and calculated GM and WM age scores for each age group (Fig. 1G). In each age group, we assessed the extent that GM and WM age scores accounted for variance in chronological age. For younger adults, the WM age score accounted for significantly less variance in chronological age than the GM age score ($R^2 = 0.24$ vs. $R^2 = 0.45$; $p < 0.003$, two-tailed, $p_{corrected} < 0.05$; Fig. 2C, Supplementary Fig. 2A). In contrast, for older adults, the GM age score accounted for significantly less variance in chronological age than the WM age score ($R^2 = 0.22$ vs. $R^2 = 0.36$; $p < 0.02$, two-tailed, $p_{corrected} < 0.05$; Fig. 2C, Supplementary Fig. 2B). In addition, for each tissue type, we assessed the extent that age scores accounted for variance in chronological age in younger and older adults. We found that the GM age score accounted for significantly more variance in chronological age in younger than older adults ($R^2 = 0.45$ vs.

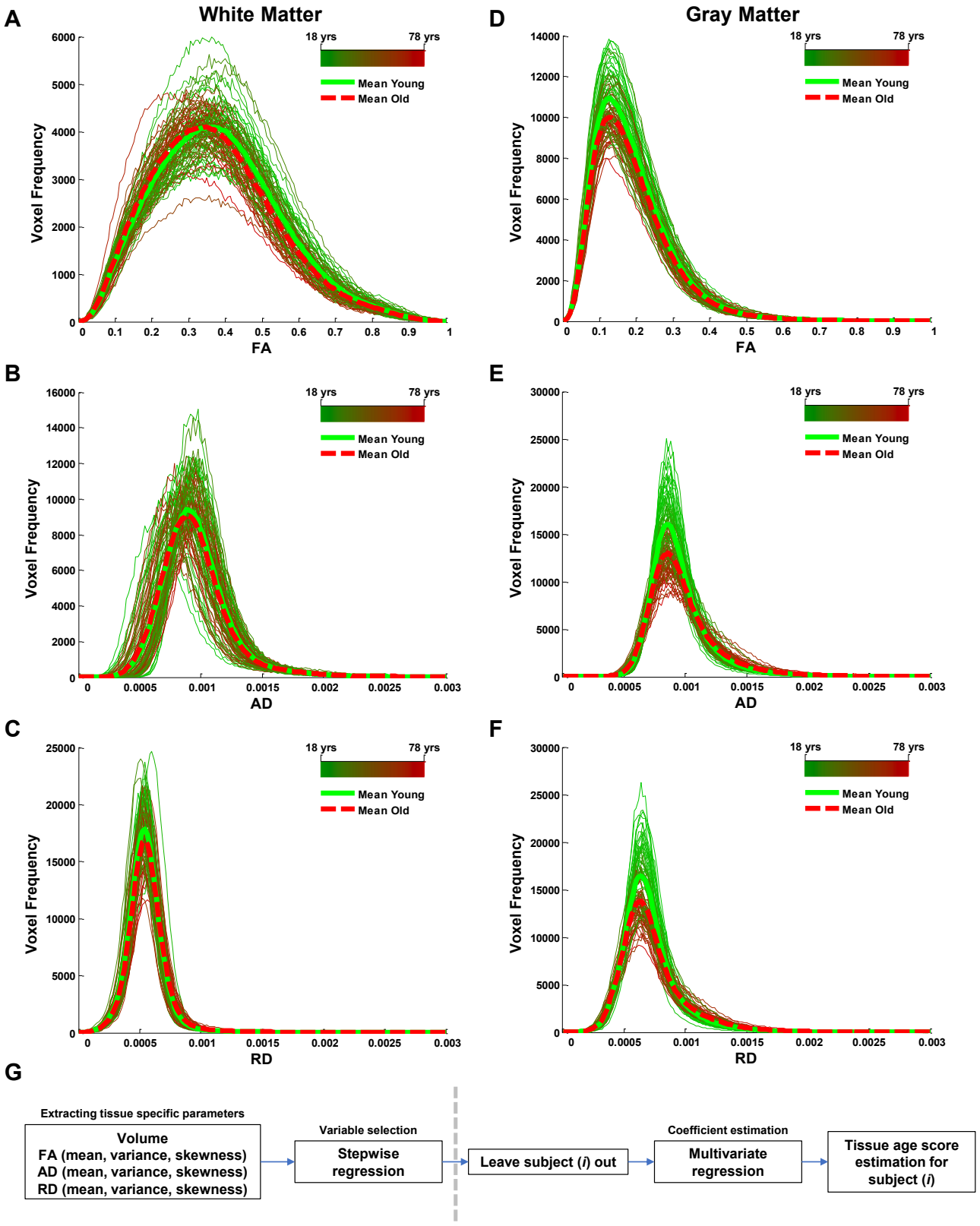

Fig. 1. Histograms of gray matter and white matter diffusion indices. The subject-level histograms (160 bins) of voxel-wise DTI measures including fractional anisotropy (FA), axial diffusivity (AD), and radial diffusivity (RD) for white matter (A–C) and gray matter (D–F). Average histograms for younger (<40 years old) and older (>40 years old) participants are also shown in solid green and dashed red lines, respectively. (G) Age-score estimation procedure. Left of the dotted line. For each tissue type, volume and distribution properties of diffusivity indices were extracted, and stepwise regression was applied to select the most relevant predictors of chronological age across all participants. Right side of the dotted line. Each participant was removed from the sample and multivariate regression of chronological age on the selected predictors was applied to estimate regression coefficients. The estimates of regression coefficients were used to derive a tissue-specific age score for the removed participant. These steps (right of the dotted line) were repeated for all participants. (For interpretation of the references to colour in this figure legend, the reader is referred to the web version of this article.)

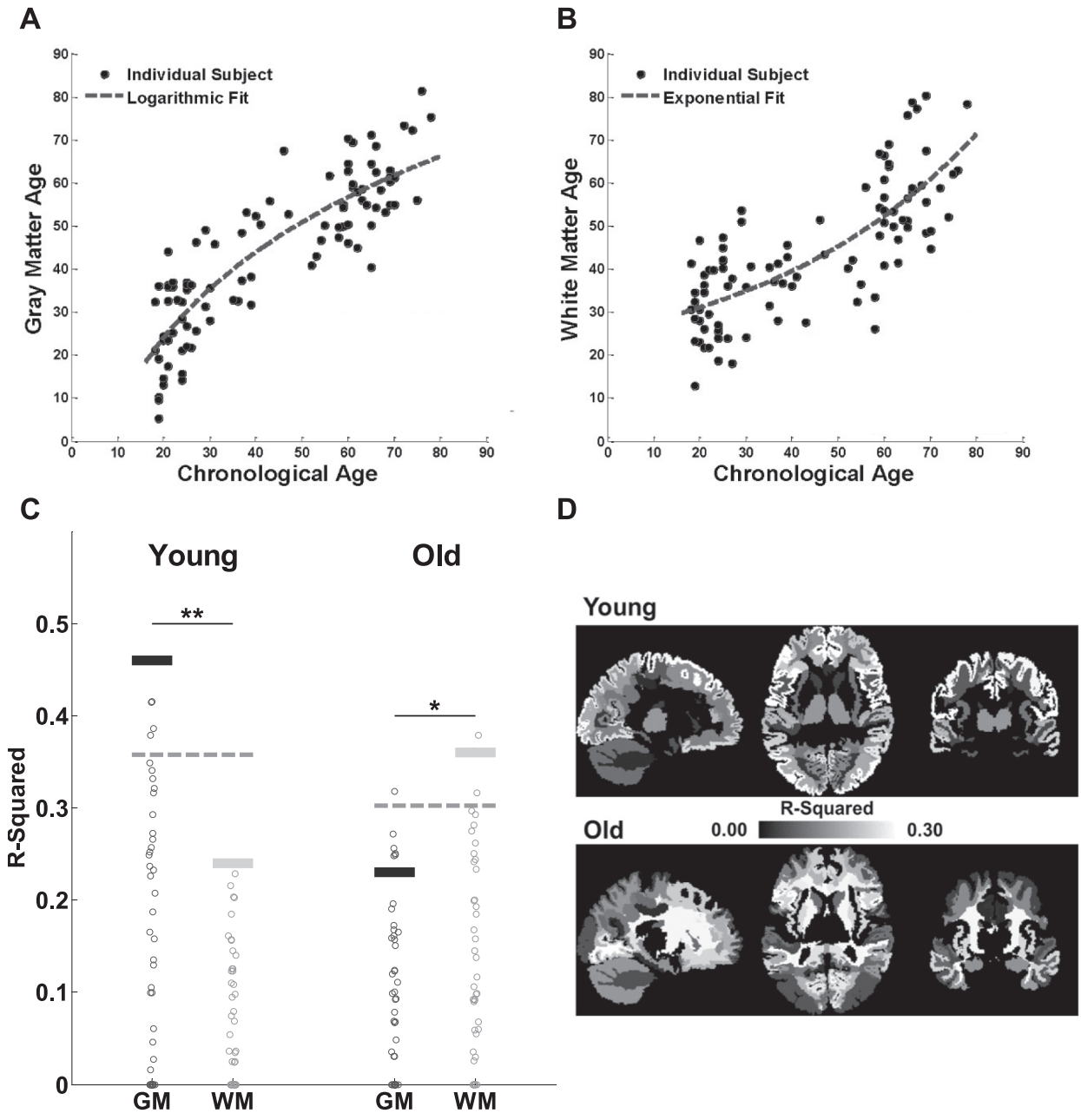

Fig. 2. Contributions of gray matter (GM) and white matter (WM) to predicting age-related differences in the brain. (A–B) The scatter plots show the GM and WM age scores (estimated using multivariate models, Fig. 1G) against the chronological age. Logarithmic, exponential, and quadratic fits (each with 3 parameters) were separately tested for the GM and WM age scores. A logarithmic function appeared to better fit the WM age scores (*RMSE* = 8.84) than quadratic (*RMSE* = 8.89) or exponential (*RMSE* = 9.25) fits, while exponential (*RMSE* = 9.95) and quadratic (*RMSE* = 9.95) functions appeared to better fit the GM age scores than a logarithmic fit (*RMSE* = 10.65). (C) R^2 of correlation between chronological and age scores obtained for GM and WM sub-regions for the younger and older adults. Each datapoint represents one region of interest. In younger adults, whole brain GM-age scores (thick dark-gray line) accounted for more of the variance in chronological age than whole brain WM-age scores (thick light-gray line, $^{**}p = 0.002$, two-tailed). In older adults, whole brain WM-age scores (thick light-gray line) accounted for more of the variance in chronological age than whole brain GM-age scores (thick dark-gray line, $^{*}p = 0.015$, two-tailed). Dashed lines show the 95-percentile of the R^2 distribution for all GM and WM sub structurers. (D) Contribution of different WM and GM sub-regions to predicting chronological age in younger (top row) versus older (bottom row) adults (see also Supplementary Tables 2 and 3). (For interpretation of the references to colour in this figure legend, the reader is referred to the web version of this article.)

$R^2 = 0.22$; $p < 0.001$, two-tailed, $p_{corrected} < 0.05$; Supplementary Fig. 2C). Meanwhile, the WM age score accounted for significantly more variance in chronological age in older than younger adults ($R^2 = 0.36$ vs. $R^2 = 0.24$; $p < 0.025$, two-tailed, $p_{corrected} < 0.05$; Supplementary Fig. 2D). These results support the position that the effect of aging on different brain tissues is different for younger and older adults and suggest a shift from larger age-related differences in GM in younger adults to larger age-related differences in WM in older adults. Notably, estimates of motion were not significantly different between the two age groups ($t(94) = 1.18$, $p = 0.24$, see Methods).

2.3. Aging in GM and WM substructures

We explored which GM and WM subs-regions showed the highest

age-related differences in younger and older adults (see Methods, Fig. 2C). In younger adults, GM structures including the postcentral gyrus, posterior cingulate, rostral anterior cingulate, and supramarginal gyrus contributed the most to these age-related differences (>95 percentile; Fig. 2D; Supplementary Table 2). In older adults, WM structures in anterior corpus callosum, and WM near fusiform and lingual gyri contributed the most to age-related differences, but also the pars opercularis of the inferior frontal gyrus in GM (>95 percentile, uncorrected; Fig. 2D; Supplementary Table 3).

2.4. Brain age and intellectual abilities

We assessed the extent to which GM and WM age scores were associated with individual differences in WASI matrix reasoning (indexing fluid intelligence: *Gf*) and WASI vocabulary (indexing crystalized intelligence: *Gc*). First, we examined age-group differences in intellectual abilities. Consistent with prior findings, younger adults outperformed older adults in *Gf* (Supplementary Table 1, $t(37) = 3.00$, $p = 0.0048$, two-tailed), and older adults outperformed younger adults in *Gc* (Supplementary Table 1, $t(37) = 2.82$, $p = 0.0077$, two-tailed). We then compared how GM and WM age scores were related to intellectual

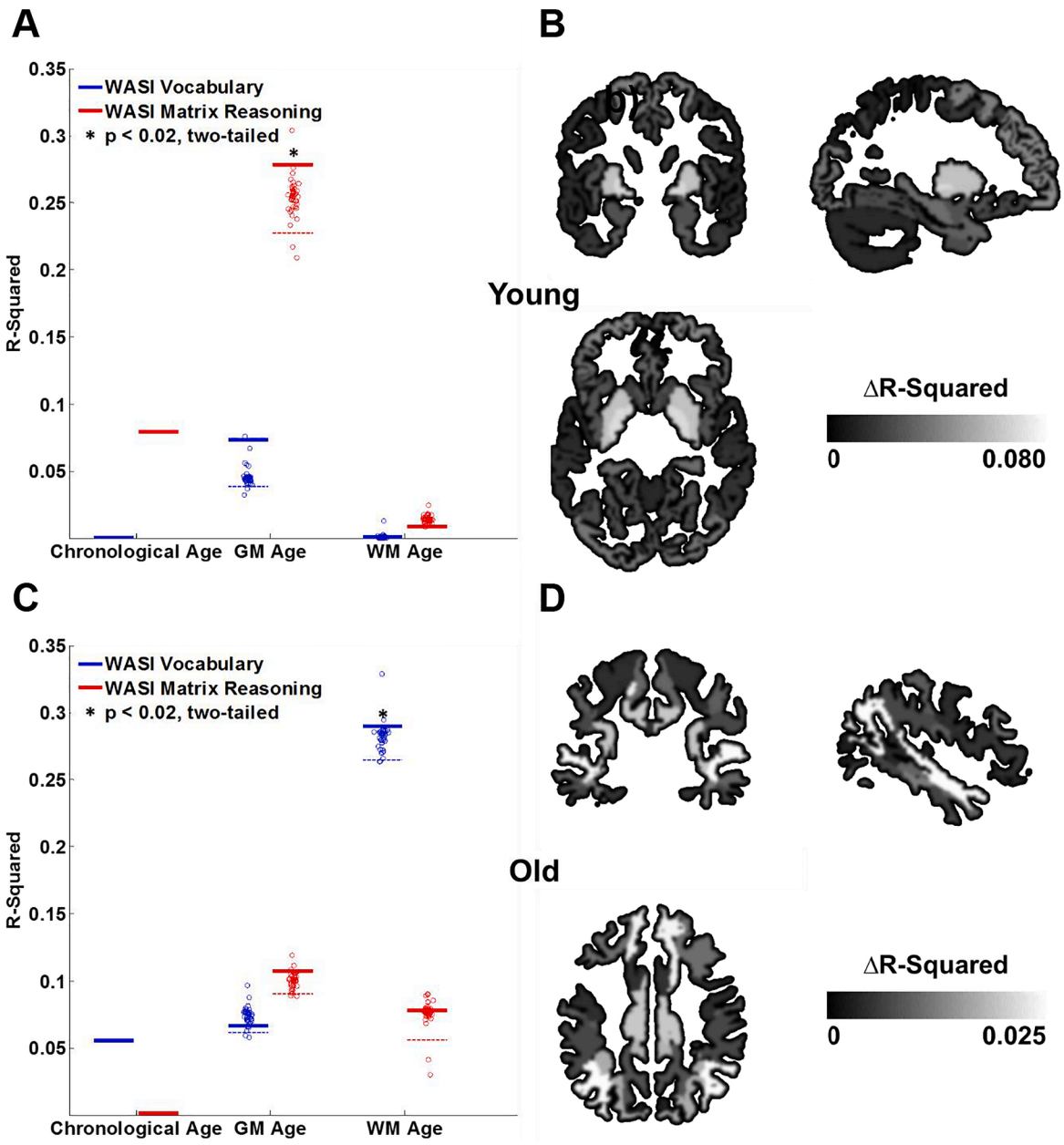

Fig. 3. Gray matter (GM) and white matter (WM) age score associations with fluid and crystallized abilities (as measured by WASI matrix reasoning and WASI vocabulary tasks, respectively) in younger and older adults. (A) Solid lines show the R^2 of the associations with intelligence measures for whole brain WM and GM age scores. The dashed lines show the 5-percentile limit for the distribution of R^2 estimates, each obtained after excluding one tissue sub-region from the analysis. A region was considered relevant when its exclusion from the model resulted in a drop in R^2 estimate below this limit. Whole-brain GM age scores significantly contributed to predicting fluid ability in younger adults ($p < 0.02$, two-tailed). (B) Putamen and pallidum GM sub-regions significantly contributed to these effects in younger adults (<5 percentile, $\Delta R^2 > 0.06$, Supplementary Table 5). (C) Whole-brain WM age scores significantly contributed to predicting crystallized ability in older adults ($p < 0.02$, two-tailed). (D) WM sub-regions nearby inferior parietal lobule and superior temporal gyrus significantly contributed to these effects in the older adults (<5 percentile, $\Delta R^2 > 0.025$, Supplementary Table 6).

abilities within age groups (Supplementary Table 4). For younger adults, only GM age scores significantly correlated with *Gf* (Fig. 3A, Supplementary Fig. 3A), where higher GM age scores were associated with lower *Gf* scores ($r(18) = -0.53$, $p = 0.017$, two-tailed). We replicated this analysis using a secondary measure of *Gf* (Supplementary Table 1) and found a similar association with GM age scores in younger adults ($r(18) = -0.55$, $p = 0.011$, two-tailed), but not with WM age scores. No such effects were observed in older adults ($p > 0.4$). For older adults, only WM age scores significantly correlated with *Gc* (Fig. 3C, Supplementary Fig. 3B). Specifically, higher WM age scores were associated with lower *Gc* ($r(17) = -0.54$, $p = 0.017$, two-tailed).

2.5. Regional associations with intelligence

Lastly, we repeated the above analysis (performed at the tissue level) for GM and WM sub-regions. We used an exploratory leave-one-out approach to characterize the contributions of individual GM and WM sub-regions to behavioral associations with brain age. We found that putamen and pallidum GM structures significantly contributed the most to *Gf* association with the GM age score in younger adults (<5 percentile, $\Delta R^2 > 0.06$, uncorrected; Fig. 3B; Supplementary Table 5). We also found that WM structures near inferior parietal lobule and superior temporal gyrus contributed the most to *Gc* association with the WM age scores in older adults (<5 percentile, $\Delta R^2 = 0.026$; Fig. 3D; Supplementary Table 6).

3. Discussion

To address our primary aim of examining tissue-specific aging patterns, the present results showed that brain WM age ($R^2 = 0.57$) and GM age ($R^2 = 0.73$) can be estimated by combining related diffusivity and volumetric measures. We showed that WM and GM are differentially sensitive to the aging process in younger versus older adults. Specifically, age-related differences in GM in younger adults were significantly larger than that in older adults ($R^2 = 0.45$ vs. $R^2 = 0.24$, Fig. 2C), whereas age-related differences in WM in older adults were significantly larger than that in younger adults ($R^2 = 0.36$ vs. $R^2 = 0.22$, Fig. 2C). Our analysis benefited from the inclusion of parameters such as variance and skewness of DTI measures which characterize the heterogeneity and bias in the whole brain FA, AD, and RD (Fig. 1). Between age groups, GM age scores accounted for more chronological age variance in younger versus older adults, whereas the WM age score accounted for higher chronological age variance in older than younger adults. Based on these observations, future longitudinal studies could investigate whether age-related GM changes precede WM changes. This pattern of results, however, is consistent with extant literature demonstrating that, whereas GM volume shows a monotonic decline across the adult lifespan, WM volume shows accelerated declines after the fourth decade of life (Ge et al., 2002b; Sowell et al., 2003).

The distinct characteristics of GM and WM aging that we observed are differentially related to fluid and crystalized abilities in younger and older adults. Despite higher fluid ability in younger than older adults, individual differences in *Gf* in younger adults were better predicted by aging effects on GM than on WM. Notably, younger individuals with higher GM age scores than their peers had lower fluid abilities. At the same time, older adults had higher *Gc* scores than younger adults and individual differences in *Gc* in older adults were best predicted by effects of age on WM than GM. That is, older individuals with higher WM age scores than their peers had lower crystalized abilities. Our results highlight age-related differences in the contributions of GM and WM to age-related differences in G*f* and G*c*, respectively. Both fluid and crystallized abilities rely on interactions between brain structures through GM and WM (Colom et al., 2009; Deary et al., 2010; Luders et al., 2009; Ritchie et al., 2015). Our results highlight the contribution of GM to age-related differences in *Gf* in younger adults that may be related to the effects of aging on neuronal populations in GM in a manner that limits their ability to process cognitively demanding functions of *Gf* (Genç et al., 2018). In contrast, the WM contribution to age-related differences in *Gc* in older adults may be driven by effects of advanced aging on integrity of axons in WM (Westlye et al., 2010) and their ability to facilitate information transfer in networks of distributed regions throughout the cortex that are involved in knowledge retrieval (Stamatakis et al., 2011). Together, these findings suggest that there may be a dissociation between the contribution of GM aging to individual differences in *Gf* in younger adults and the contribution of WM aging to individual differences in *Gc* in older adults. Given the cross-sectional nature of our study, we cannot address how measures of brain structure and intelligence may change and influence one another over age. Thus, generalizability of our findings requires longitudinal data to determine the trajectories of GM and WM aging patterns over the life span and to further investigate their relationship to changes in G*f* and G*c*.

Given the regional differences in effects of aging on GM and WM (Kochunov et al., 2007; Pfefferbaum et al., 2010; Sexton et al., 2014), we further characterized age-related sensitivity across multiple regions of interest for both tissues types and estimated their contribution to the associations with intellectual abilities. Results revealed that areas within the frontoparietal network (implicated in *Gf*) (Jung and Haier, 2007) show the highest age-related differences in GM in younger adults. In addition, we found that the putamen and pallidum were most important for the association between GM age scores and *Gf*. Considering the action of multiple neurotransmitters in putamen and pallidum and their diverse anatomical projections to the cortex, these structures may serve as key gateways for functions related to *Gf* (Burgaleta et al., 2014; Rhein et al., 2014; Rypma et al., 1999). The importance of the inferior parietal lobule and superior temporal gyrus for the associations between WM age scores and *Gc* (Supplementary Table 6) is consistent with the recognized role of these regions in memory and language processing (Bigler et al., 2007; O'Connor et al., 2010). It is important to point out that our study was limited to measuring *Gf* and *Gc* using a limited set of psychometric tests in a notably small sample. Moreover, some of our diffusivity measures may be influenced by the presence of iron, which accumulates in select basal ganglia nuclei (including the putamen and pallidum) across the adult life span (Langley et al., 2019). Future work utilizing latent factors of behavioral measures in a larger sample and with improved image acquisition and distortion correction approaches (Yamada et al., 2014) is needed to assess the validity of our results.

Age-related differences in brain structures have been of interest since neuroimaging has become widely accessible (Coffey et al., 1992; Meyer et al., 1994). Advances in methodological approaches have led different research groups to provide estimates of brain age with high accuracy using volumetric or morphometric variables that are derived from structural data (e.g., T1-weighted images) (Beheshti et al., 2019; Cole et al., 2017b; Franke et al., 2010). Multimodal approaches that, for example, integrate diffusivity and volumetric characteristics have been helpful for studying the interacting effects of aging and neuropsychiatric disorders on the brain (Shahab et al., 2019) and have improved the predictions of brain age (Niu et al., 2020). Our multimodal approach involved identifying age-related measures of macrostructure (i.e., volume) and microstructure (i.e., distribution properties of DTI data) to study cross-sectional age-related differences in GM and WM. Results revealed that AD and RD indices in GM were significant predictors of age, particularly in younger adults. Across the adult life span, when combined with volumetric measures, the GM age score accounted for about 74% of chronological age variance (mean error of 8.39 years in predicting chronological age). DTI measures have been assessed within GM structures in aging and neuropsychiatric disorders (Müller et al., 2006; Nazeri et al., 2017; Venkatesh et al., 2020). Age-related differences in GM diffusivity may reflect a composite of changes in glial cell bodies, dendrites, and axonal-dendritic terminal density (Abdelkarim et al., 2019; Kim et al., 2013) that may affect the quality of proximal intercellular connectivity due to reductions in dendritic arborization or

spine numbers (Fukutomi et al., 2019; Hof and Morrison, 2004; Peters, 2002). Notably, our results suggsted that volumetric measures alone may not be able to fully capture age-related differences in GM. For WM, age-related differences were more pronounced later in our sample (>40 year), primarily affecting FA (as well as AD and RD), possibly due to factors such as axonal degeneration, demyelination, and gliosis (Bennett et al., 2010; Kraus et al., 2007; Peters, 2009). Though the median age in our sample was 40 years old, prior work has indicated this age may be a pivotal point for aging of WM and GM. Specifically, decreases in GM density that were accompanied by increases in WM volume before age 40 (Ge et al., 2002b), have been suggested to reflect increases in myelination, while degenerative processes have been linked to GM volume decline after age 40 (Sowell et al., 2003). However, there are indications that WM volumetric increases peak at the fifth decade of life, while thickening in GM structures such as inferior parietal and posterior temporal regions is inversed following the fifth decade of life (Sowell et al., 2003; Tau and Peterson, 2010). It is noteworthy that cerebrospinal fluid volume is another important contributor to age-related differences in the brain which we did not assess in this paper (Levakov et al., 2020). Our approach of estimating brain age relied on selecting most relevant distribution properties of diffusivity measures that was presumably robust to heterogeneity in the effect of aging on brain regions. Future research on brain age estimation may compare our approach with other approaches that rely on extracting the mean of structural (or functional) measures from regions of interest (Niu et al., 2020). Future work should also investigate the shared and unique age-related variance in structural properties of GM and WM and incorporate additional measures of myelination and morphometry in multivariate models of brain age.

4. Conclusion

By introducing a composite index of macrostructural and microstructural properties, we derived estimates of brain age (age scores) for GM and WM and reported different effects of age on these tissue types. We provided evidence that relative to volumetric measures, distribution properties of diffusivity indices accounted for distinct age-related variance in both GM and WM. GM showed higher age-related differences in younger than older adults whereas WM showed higher age-related differences in older than younger adults. We also showed that age-related differences in GM and WM may have implications for predicting *Gf* and G*c*, respectively. The GM age score was significantly associated with *Gf* in younger adults, whereas the WM age score was significantly associated with *Gc* in older adults. Prominent theories of aging suggest that changes over the adult life span are intrinsic, progressive, and deleterious (Viña et al., 2007) and may reflect a complex set of responses (Goh and Park, 2009; Rypma and D'Esposito, 2000) to damage and error in cellular mechanisms (Abdelkarim et al., 2019; Jin, 2010). Our results may be informative for characterizing cross-sectional effects of age on different brain tissues and may have implications for future research on the shift from excelling at novel problems solving (*Gf*) in younger adults to the state of specializing and succeeding in recruiting past knowledge and experience (*Gc*) in older adults. Future work may also assess the extent to which these observations form the basis of an aging model in which cognitive flexibility in younger adults coupled with stores of knowledge and experience gained by older adults could result in enhanced productivity across generations (Kaplan et al., 2000). Finally, our measures of brain aging may have implications for diagnosis and monitoring of age-related brain disorders that differentially affect WM and GM such as Alzheimer's disease.

5. Methods and materials

5.1. Participants

100 individuals were recruited for this study (18–78 years old). Three individuals were excluded due to distorted structural data ($n = 1$), abnormal findings in the white matter ($n = 1$), and excessive motion during the DTI scan ($n = 1$). Participants ($n = 97$, age = 43.47 ± 19.65 years old, 58 females) had at least a high school degree and had normal or corrected-to-normal vision. Participants were recruited through the University of Texas at Dallas and from local, online, and newspaper advertising. All participants performed within the age-expected range (scores ≥ 26) on 2 brief measures used to screen for general cognitive functioning: the Mini Mental State Examination (Folstein et al., 1975) and Telephone Interview for Cognitive Status (Brandt et al., 1988). Informed consent was obtained from participants and they received either payment or course credit for their participation. The University of Texas at Dallas Institutional Review Board approved the experimental procedures. Prior to participation, individuals were screened for conditions that would prevent them from being able to enter the magnetic resonance imaging (MRI) scanner (e.g., being pregnant, having ferrous metal implants, having difficulty lying in the supine position for 30 min, and being claustrophobic), or influence their cognitive functioning and/or contribute to brain pathology (e.g., history of stroke, dementia, diabetes, and unmanaged depression or hypertension).

5.2. Measures of intelligence

Intelligence was measured using standardized WASI vocabulary test for crystalized intelligence (*Gc*) and WASI matrix reasoning for fluid intelligence (*Gf*) (Wechsler, 1999) (Supplementary Table 1). These measures were only available in 20 younger and 19 older participants, though our prior work has shown age-related effects on the association between behavior and DTI indices in a comparable sample size (Bennett et al., 2012). A secondary measure of fluid intelligence included a composite of *z*-scores of WAIS-III Symbol Search (# correct - # incorrect), WAIS-III Digit Span total, and Trail Making B tests, which indexed processing speed, working memory, and executive functioning of fluid abilities, respectively (Reitan and Wolfson, 1985; Tulsky et al., 2003). No adjustments for age were carried out for comparisons with the imaging measures.

5.3. Scanning protocol

MRI images were acquired using a Philips Achieva 3.0 Tesla MRI system (Philips Medical System, The Netherlands) at the Advanced Imaging Research Center at the University of Texas Southwestern Medical Center. Participants lay in the supine position in the scanner with an 8-element, SENSE, receive-only head coil. Fitted padding was used to minimize head movements. For structural MR, a high resolution T1-weighted MPRAGE image was acquired with the following parameters: scan time = 237 s, TR = 8.1 ms, TE = 3.7 ms, flip angle = 12°, FOV = 256 × 256 × 160 mm^3, spatial resolution = 1-mm isotropic, and 160 sagittal slices. A diffusion weighted echo planar imaging sequence was acquired using gradient values of b = 0 (one image) and b = 1000 s/mm^2 (applied in 30 directions) and the following parameters: scan time = 265 s, TR = 5630 ms, TE = 51 ms, 65 axial interleaved slices (2.2 mm slice thickness, no gap), acquisition matrix = 112 × 112 (2 mm in-plane resolution) reconstructed at 256 × 256.

5.4. DTI preprocessing

Diffusion-weighted data were processed using the University of Oxford's Center for Functional Magnetic Resonance Imaging of the Brain (FMRIB) Software Library (FSL) release 4.0 (http://www.fmrib.ox.ac.uk/fsl). The first volume that did not have gradient applied (b = 0) was used to generate a binary brain mask with the 'bet' function in FSL. Subject movements and eddy current-induced distortions were corrected using the 'eddy_correct' function in FSL. Estimates of displacement relative to the first image were computed using the alignment parameters obtained from the motion correction step. One participant with mean relative displacement of 2.46 mm (>10 × SD) was excluded

from the sample (as mentioned in the Participants section). Mean estimates of relative displacement were not significantly different between the younger and older participants, split at age 40 years ($M_{young} = 0.58$ mm, $SD_{young} = 0.12$ mm; $M_{old} = 0.61$ mm, $SD_{old} = 0.13$ mm; $t(94) = 1.18$, $p = 0.24$, two-tailed). Finally, the 'dtifit' function in FSL was used to independently fit diffusion tensors to each voxel, with the brain mask limiting the fitting of tensors to brain space. The output yielded voxel-wise maps of FA, AD (the primary direction of diffusion), and RD (calculated as the average of the two non-primary diffusion directions).

5.5. Anatomical data processing

Cortical and subcortical segmentations were performed using FreeSurfer v5.1 in the subject-space (Martinos Center for Biomedical Imaging, Charlestown, Massachusetts, USA; https://surfer.nmr.mgh.harvard.edu/fswiki). The generated segmentations were inspected relative to the structural MR image for quality assurance. When necessary, the volumes were edited to ensure alignment with brain boundaries as suggested by the FreeSurfer manual. The 'wmparc' FreeSurfer output file was used to create a single GM mask (including cortical, subcortical and cerebellar regions) and a single WM mask (including cerebrum and cerebellar regions) for each participant. In addition, 'wmparc' was used to extract 43 bilateral GM regions and 41 bilateral WM regions for each subject for the regional analyses. It is noteworthy that absolute estimates of regional volumes are different across FreeSurfer versions, but analyses that relied on the relative difference between regional volumes such as correlations between regional volumes and age were preserved within FreeSurfer versions (Bigler et al., 2020). For each participant, the skull-stripped anatomical brain was aligned with an affine transformation to the diffusion data using the 'flirt' function in FSL. The same transformation parameters were applied to the GM and WM masks. Finally, the masks were resampled to match the resolution of DTI. All images were visually inspected to ensure proper alignment between anatomical masks and DTI maps.

5.6. WM and GM age scores

A total of 10 regressors were initially included in the analysis for each tissue type. Specifically, from the anatomical masks of GM and WM, a measure of total volume was calculated for each tissue type (or region) in the subject space (1 regressor). For the DTI data, within anatomical mask of each tissue (or sub-region) measures of mean, variance, and skewness were calculated for FA, AD, and RD distributions in the subject space (9 regressors) (Fig. 1A–F) in MATLAB (The MathWorks Inc., Natick, MA). We included variance which represented relative spread (indexing heterogeneity) of the whole-tissue distribution in diffusivity indices and included skewness which represented asymmetry (bias) in the data away from the mean. Fig. 1G shows a schematic view of our procedure for estimating tissue-specific age scores. For each tissue type, we performed an initial stepwise regression of chronological age on all 10 regressors to select tissue-specific age-related regressors using data from the entire cohort (or when indicated for each age group). This dimension reduction was performed to alleviate multicollinearity between the regressors (Graham, 2003). Stepwise regression was performed in MATLAB using the 'stepwisefit' function with the default settings ($p_{enter} = 0.05$, $p_{remove} = 0.1$, no initial fit specified). Next, we removed one participant from the sample, and used a full multivariate regression of chronological age on the selected regressors to estimate regressor coefficients. This was done to obtain unbiased estimates of regressor coefficients and to alleviate the data overfitting problem due to presence of multiple regressors (Hawkins, 2004). Finally, these regressor coefficients were used to estimate a tissue-specific age score for the removed participant. This procedure was repeated for all participants (Fig. 1G). The common variance (R^2) between chronological age and the tissue-specific age scores were computed to index the quality of fit. We also repeated the variable selection step with lasso regression in MATLAB using 20-fold cross-validation to find the sparsest model that was within one standard error of the minimum mean square error (Tibshirani, 1996) (see Supplementary Results and Supplementary Fig. 1). For the regional analyses, a similar procedure was performed (as shown in Fig. 1G) where volume and distribution properties of diffusivity indices were extracted for each of GM and WM sub-regions identified in 'wmparc' (see Anatomical data processing).

Acknowledgments

This study was supported by Friends of BrainHealth Distinguished New Scientist Award (E.S-K.), and NIH grants R01 AG029523 (B.R.), R01 AG047972 (B.R.), and F32 AG038299 (I.J.B.). We thank Amanda Colby, Nicholas Hubbard, Michael Kriegsman, Meghana Karnik-Henry, Michael Motes, and Neena Rao who assisted in various aspects of this work.

Author contributions

E.S-K. initiated the study, developed the techniques, and performed the analyses. ESK wrote the paper with contributions from I.J.B. and B.R. B.R. and I.J.B. designed experiments and supervised data collection. Z.T. assisted with data processing and quality control. D.C.K. edited the paper and reviewed the analyses. All authors commented on the manuscript.

Data availability

The data that support the findings of this study are available from the corresponding author upon reasonable request.

Appendix A. Supplementary data

Supplementary data to this article can be found online at https://doi.org/10.1016/j.brainres.2021.147431.

References

Abdelkarim, D., Zhao, Y., Turner, M.P., Sivakolundu, D.K., Lu, H., Rypma, B., 2019. A neural-vascular complex of age-related changes in the human brain: Anatomy, physiology, and implications for neurocognitive aging. Neurosci. Biobehav. Rev. 107, 927–944.

Abe, O., Yamasue, H., Aoki, S., Suga, M., Yamada, H., Kasai, K., Masutani, Y., Kato, N., Kato, N., Ohtomo, K., 2008. Aging in the CNS: comparison of gray/white matter volume and diffusion tensor data. Neurobiol. Aging 29, 102–116.

Anatürk, M., Demnitz, N., Ebmeier, K.P., Sexton, C.E., 2018. A systematic review and meta-analysis of structural magnetic resonance imaging studies investigating cognitive and social activity levels in older adults. Neurosci. Biobehav. Rev. 93, 71–84.

Beheshti, I., Gravel, P., Potvin, O., Dieumegarde, L., Duchesne, S., 2019. A novel patch-based procedure for estimating brain age across adulthood. Neuroimage. 197, 618–624.

Bender, A.R., Völkle, M.C., Raz, N., 2016. Differential aging of cerebral white matter in middle-aged and older adults: A seven-year follow-up. NeuroImage. 125, 74–83.

Benedetti, B., Charil, A., Rovaris, M., Judica, E., Valsasina, P., Sormani, M., Filippi, M., 2006. Influence of aging on brain gray and white matter changes assessed by conventional, MT, and DT MRI. Neurology. 66, 535–539.

Bennett, I.J., Madden, D.J., Vaidya, C.J., Howard, D.V., Howard, J.H., 2010. Age-related differences in multiple measures of white matter integrity: A diffusion tensor imaging study of healthy aging. Hum. Brain Mapp. 31, 378–390.

Bennett, I.J., Motes, M.A., Rao, N.K., Rypma, B., 2012. White matter tract integrity predicts visual search performance in young and older adults. Neurobiol. Aging 33, 433.e21–433.e31.

Bennett, I.J., Rypma, B., 2013. Advances in functional neuroanatomy: A review of combined DTI and fMRI studies in healthy younger and older adults. Neurosci. Biobehav. Rev. 37, 1201–1210.

Benson, R.R., Meda, S.A., Vasudevan, S., Kou, Z., Govindarajan, K.A., Hanks, R.A., Millis, S.R., Makki, M., Latif, Z., Coplin, W., Meythaler, J., Haacke, E.M., 2007. Global white matter analysis of diffusion tensor images is predictive of injury severity in traumatic brain injury. J Neurotrauma. 24, 446–459.

Bigler, E.D., Mortensen, S., Neeley, E.S., Ozonoff, S., Krasny, L., Johnson, M., Lu, J., Provencal, S.L., McMahon, W., Lainhart, J.E., 2007. Superior temporal gyrus, language function, and autism. Develop. Neuropsychol. 31, 217–238.

Bigler, E.D., Skiles, M., Wade, B.S.C., Abildskov, T.J., Tustison, N.J., Scheibel, R.S., Newsome, M.R., Mayer, A.R., Stone, J.R., Taylor, B.A., Tate, D.F., Walker, W.C., Levin, H.S., Wilde, E.A., 2020. FreeSurfer 5.3 versus 6.0: are volumes comparable? A Chronic Effects of Neurotrauma Consortium study. Brain Imaging Behav. 14, 1318–1327.
Brandt, J., Spencer, M., Folstein, M., 1988. The telephone interview for cognitive status. Cognitive Behav. Neurol. 1, 111–118.
Burgaleta, M., MacDonald, P.A., Martínez, K., Roman, F.J., Álvarez-Linera, J., Gonzalez, A.R., Karama, S., Colom, R., 2014. Subcortical regional morphology correlates with fluid and spatial intelligence. Hum. Brain Mapp. 35, 1957–1968.
Charlton, R., Schiavone, F., Barrick, T., Morris, R., Markus, H., 2010. Diffusion tensor imaging detects age related white matter change over a 2 year follow-up which is associated with working memory decline. J. Neurol. Neurosurg. Psychiatry 81, 13–19.
Charlton, R.A., Barrick, T.R., McIntyre, D.J., Shen, Y., O'Sullivan, M., Howe, F.A., Clark, C.A., Morris, R.G., Markus, H.S., 2006. White matter damage on diffusion tensor imaging correlates with age-related cognitive decline. Neurology. 66, 217–222.
Chen, P.-Y., Chen, C.-L., Hsu, Y.-C., Tseng, W.-Y.-I., 2020. Fluid intelligence is associated with cortical volume and white matter tract integrity within multiple-demand system across adult lifespan. NeuroImage 116576.
Chiapponi, C., Piras, F., Piras, F., Fagioli, S., Caltagirone, C., Spalletta, G., 2013. Cortical grey matter and subcortical white matter brain microstructural changes in schizophrenia are localised and age independent: A case-control diffusion tensor imaging Study. PLoS One 8, e75115.
Coffey, C.E., Wilkinson, W.E., Parashos, L., Soady, S.A.R., Sullivan, R.J., Patterson, L.J., Figiel, G.S., Webb, M.C., Spritzer, C.E., Djang, W.T., 1992. Quantitative cerebral anatomy of the aging human brain. A cross-sectional study using magnetic resonance imaging. 42, 527, 527.
Cole, J., Ritchie, S., Bastin, M., Hernández, M.V., Maniega, S.M., Royle, N., Corley, J., Pattie, A., Harris, S., Zhang, Q., 2017a. Brain age predicts mortality. Mol. Psychiatry.
Cole, J.H., Poudel, R.P., Tsagkrasoulis, D., Caan, M.W., Steves, C., Spector, T.D., Montana, G., 2017b. Predicting brain age with deep learning from raw imaging data results in a reliable and heritable biomarker. NeuroImage. 163, 115–124.
Colom, R., Haier, R.J., Head, K., Álvarez-Linera, J., Quiroga, M.Á., Shih, P.C., Jung, R.E., 2009. Gray matter correlates of fluid, crystallized, and spatial intelligence: Testing the P-FIT model. Intelligence. 37, 124–135.
Colom, R., Karama, S., Jung, R.E., Haier, R.J., 2010. Human intelligence and brain networks. Dialogues Clin. Neurosci. 12, 489.
de la Plata, C.D.M., Yang, F.G., Wang, J.Y., Krishnan, K., Bakhadirov, K., Paliotta, C., Aslan, S., Devous, M.D., Moore, C., Harper, C., 2011. Diffusion tensor imaging biomarkers for traumatic axonal injury: Analysis of three analytic methods. J. Int. Neuropsychol. Soc. 17, 24–35.
de Mooij, S.M., Henson, R.N., Waldorp, L.J., Kievit, R.A., 2018. Age differentiation within gray matter, white matter, and between memory and white matter in an adult life span cohort. J. Neurosci. 38, 5826–5836.
Deary, I.J., Penke, L., Johnson, W., 2010. The neuroscience of human intelligence differences. Nat. Rev. Neurosci. 11, 201–211.
Della Nave, R., Foresti, S., Pratesi, A., Ginestroni, A., Inzitari, M., Salvadori, E., Giannelli, M., Diciotti, S., Inzitari, D., Mascalchi, M., 2007. Whole-brain histogram and voxel-based analyses of diffusion tensor imaging in patients with leukoaraiosis: Correlation with motor and cognitive impairment. Am. J. Neuroradiol. 28, 1313–1319.
Farokhian, F., Yang, C., Beheshti, I., Matsuda, H., Wu, S., 2017. Age-related gray and white matter changes in normal adult brains. Aging Disease 8, 899.
Folstein, M.F., Folstein, S.E., McHugh, P.R., 1975. "Mini-mental state": A practical method for grading the cognitive state of patients for the clinician. J. Psychiatr. Res. 12, 189–198.
Foster, J.C., Taylor, G.A., 1920. The applicability of mental tests to persons over fifty years of age. J. Appl. Psychol. 4, 39–58.
Franke, K., Ziegler, G., Klöppel, S., Gaser, C., Initiative, A.s.D.N., 2010. Estimating the age of healthy subjects from T1-weighted MRI scans using kernel methods: Exploring the influence of various parameters. Neuroimage. 50, 883–892.
Fukutomi, H., Glasser, M.F., Murata, K., Akasaka, T., Fujimoto, K., Yamamoto, T., Autio, J.A., Okada, T., Togashi, K., Zhang, H., Van Essen, D.C., Hayashi, T., 2019. Diffusion tensor model links to neurite orientation dispersion and density imaging at high b-value in cerebral cortical gray matter. Sci. Rep. 9, 12246.
Ge, Y., Grossman, R.I., Babb, J.S., Rabin, M.L., Mannon, L.J., Kolson, D.L., 2002a. Age-related total gray matter and white matter changes in normal adult brain. Part II: Quantitative magnetization transfer ratio histogram analysis. Am. J. Neuroradiol. 23, 1334–1341.
Ge, Y., Grossman, R.I., Babb, J.S., Rabin, M.L., Mannon, L.J., Kolson, D.L., 2002b. Age-related total gray matter and white matter changes in normal adult brain. Part I: volumetric MR imaging analysis. Am. J. Neuroradiol. 23, 1327–1333.
Genç, E., Fraenz, C., Schlüter, C., Friedrich, P., Hossiep, R., Voelkle, M.C., Ling, J.M., Güntürkün, O., Jung, R.E., 2018. Diffusion markers of dendritic density and arborization in gray matter predict differences in intelligence. Nat. Commun. 9, 1905.
Goh, J.O., Park, D.C., 2009. Neuroplasticity and cognitive aging: The scaffolding theory of aging and cognition. Restor. Neurol. Neurosci. 27, 391–403.
Góngora, D., Vega-Hernández, M., Jahanshahi, M., Valdés-Sosa, P.A., Bringas-Vega, M.L., CHBMP, 2020. Crystallized and fluid intelligence are predicted by microstructure of specific white-matter tracts. Hum. Brain Mapp. 41, 906–916.
Graham, M.H., 2003. Confronting multicollinearity in ecological multiple regression. Ecology 84, 2809–2815.
Grydeland, H., Walhovd, K.B., Tamnes, C.K., Westlye, L.T., Fjell, A.M., 2013. Intracortical myelin links with performance variability across the human lifespan: results from T1- and T2-weighted MRI myelin mapping and diffusion tensor imaging. J. Neurosci. 33, 18618–18630.
Hawkins, D.M., 2004. The problem of overfitting. J. Chem. Inf. Comput. Sci. 44, 1–12.
Hof, P.R., Morrison, J.H., 2004. The aging brain: morphomolecular senescence of cortical circuits. Trends Neurosci. 27, 607–613.
Jin, K., 2010. Modern biological theories of aging. Aging Disease 1, 72.
Jung, R.E., Haier, R.J., 2007. The Parieto-Frontal Integration Theory (P-FIT) of intelligence: Converging neuroimaging evidence. Behav. Brain Sci. 30, 135–154.
Kaplan, H., Hill, K., Lancaster, J., Hurtado, A.M., 2000. A theory of human life history evolution: Diet, intelligence, and longevity. Evol. Anthropol.: Issues, News, Rev. 9, 156–185.
Kennedy, K.M., Raz, N., 2009. Pattern of normal age-related regional differences in white matter microstructure is modified by vascular risk. Brain Res. 1297, 41–56.
Kim, H.J., Kim, S.J., Kim, H.S., Choi, C.G., Kim, N., Han, S., Jang, E.H., Chung, S.J., Lee, C.S., 2013. Alterations of mean diffusivity in brain white matter and deep gray matter in Parkinson's disease. Neurosci. Lett. 550, 64–68.
Kochunov, P., Thompson, P.M., Lancaster, J.L., Bartzokis, G., Smith, S., Coyle, T., Royall, D.R., Laird, A., Fox, P.T., 2007. Relationship between white matter fractional anisotropy and other indices of cerebral health in normal aging: Tract-based spatial statistics study of aging. NeuroImage. 35, 478–487.
Kochunov, P., Glahn, D.C., Lancaster, J., Thompson, P.M., Kochunov, V., Rogers, B., Fox, P., Blangero, J., Williamson, D.E., 2011. Fractional anisotropy of cerebral white matter and thickness of cortical gray matter across the lifespan. NeuroImage. 58, 41–49.
Kraus, M.F., Susmaras, T., Caughlin, B.P., Walker, C.J., Sweeney, J.A., Little, D.M., 2007. White matter integrity and cognition in chronic traumatic brain injury: A diffusion tensor imaging study. Brain. 130, 2508–2519.
Langley, J., Hussain, S., Flores, J.J., Bennett, I.J., Hu, X., 2019. Characterization of age-related microstructural changes in locus coeruleus and substantia nigra pars compacta. Neurobiol. Aging.
Levakov, G., Rosenthal, G., Shelef, I., Raviv, T.R., Avidan, G., 2020. From a deep learning model back to the brain—Identifying regional predictors and their relation to aging. Hum. Brain Mapp.
Luders, E., Narr, K.L., Thompson, P.M., Toga, A.W., 2009. Neuroanatomical correlates of intelligence. Intelligence. 37, 156–163.
Madan, C.R., Kensinger, E.A., 2018. Predicting age from cortical structure across the lifespan. Eur. J. Neuroscience.
Meyer, J.S., Takashima, S., Terayama, Y., Obara, K., Muramatsu, K., Weathers, S., 1994. CT changes associated with normal aging of the human brain. J. Neurol. Sci. 123, 200–208.
Michielse, S., Coupland, N., Camicioli, R., Carter, R., Seres, P., Sabino, J., Malykhin, N., 2010. Selective effects of aging on brain white matter microstructure: A diffusion tensor imaging tractography study. Neuroimage. 52, 1190–1201.
Müller, M., Mazanek, M., Weibrich, C., Dellani, P., Stoeter, P., Fellgiebel, A., 2006. Distribution characteristics, reproducibility, and precision of region of interest–based hippocampal diffusion tensor imaging measures. Am. J. Neuroradiol. 27, 440–446.
Nazeri, A., Chakravarty, M.M., Rotenberg, D.J., Rajji, T.K., Rathi, Y., Michailovich, O.V., Voineskos, A.N., 2015. Functional consequences of neurite orientation dispersion and density in humans across the adult lifespan. J. Neurosci. 35, 1753–1762.
Nazeri, A., Mulsant, B.H., Rajji, T.K., Levesque, M.L., Pipitone, J., Stefanik, L., Shahab, S., Roostaei, T., Wheeler, A.L., Chavez, S., Voineskos, A.N., 2017. Gray Matter Neuritic Microstructure Deficits in Schizophrenia and Bipolar Disorder. Biol. Psychiatry 82, 726–736.
Nestor, P.G., Nakamura, M., Niznikiewicz, M., Levitt, J.J., Newell, D.T., Shenton, M.E., McCarley, R.W., 2015. Attentional Control and Intelligence: MRI Orbital Frontal Gray Matter and Neuropsychological Correlates. Behav. Neurol. 2015, 354186.
Niu, X., Zhang, F., Kounios, J., Liang, H., 2020. Improved prediction of brain age using multimodal neuroimaging data. Hum. Brain Mapp. 41, 1626–1643.
O'Connor, A.R., Han, S., Dobbins, I.G., 2010. The inferior parietal lobule and recognition memory: Expectancy violation or successful retrieval? J. Neurosci. 30, 2924–2934.
Ohtani, T., Nestor, P.G., Bouix, S., Newell, D., Melonakos, E.D., McCarley, R.W., Shenton, M.E., Kubicki, M., 2017. Exploring the neural substrates of attentional control and human intelligence: Diffusion tensor imaging of prefrontal white matter tractography in healthy cognition. Neuroscience 341, 52–60.
Pareek, V., Rallabandi, V.S., Roy, P.K., 2018. A correlational study between microstructural white matter properties and macrostructural gray matter volume across normal ageing: Conjoint DTI and VBM Analysis. Magnetic Resonance Insights. 11, 1178623X18799926.
Penke, L., Maniega, S.M., Bastin, M., Hernández, M.V., Murray, C., Royle, N., Starr, J., Wardlaw, J., Deary, I., 2012. Brain white matter tract integrity as a neural foundation for general intelligence. Mol. Psychiatry 17, 1026–1030.
Peters, A., 2002. Structural changes that occur during normal aging of primate cerebral hemispheres. Neurosci. Biobehav. Rev. 26, 733–741.
Peters, A., 2009. The effects of normal aging on myelinated nerve fibers in monkey central nervous system. Front Neuroanat. 3, 11.
Pfefferbaum, A., Adalsteinsson, E., Rohlfing, T., Sullivan, E.V., 2010. Diffusion tensor imaging of deep gray matter brain structures: effects of age and iron concentration. Neurobiol. Aging 31, 482–493.
Pfefferbaum, A., Sullivan, E.V., 2015. Cross-sectional versus longitudinal estimates of age-related changes in the adult brain: overlaps and discrepancies. Neurobiol. Aging 36, 2563–2567.

Rathee, R., Rallabandi, V.S., Roy, P.K., 2016. Age-related differences in white matter integrity in healthy human brain: evidence from structural MRI and diffusion tensor imaging. Magnetic Resonance Insights. 9, S39666.
Raz, N., Lindenberger, U., Rodrigue, K.M., Kennedy, K.M., Head, D., Williamson, A., Dahle, C., Gerstorf, D., Acker, J.D., 2005. Regional brain changes in aging healthy adults: General trends, individual differences and modifiers. Cereb. Cortex 15, 1676–1689.
Reitan, R.M., Wolfson, D., 1985. The Halstead-Reitan neuropsychological test battery: Theory and clinical interpretation. Vol. 4, Reitan Neuropsychology.
Rhein, C., Mühle, C., Richter-Schmidinger, T., Alexopoulos, P., Doerfler, A., Kornhuber, J., 2014. Neuroanatomical Correlates of Intelligence in Healthy Young Adults: The Role of Basal Ganglia Volume. PLoS One 9, e93623.
Ritchie, S.J., Bastin, M.E., Tucker-Drob, E.M., Maniega, S.M., Engelhardt, L.E., Cox, S.R., Royle, N.A., Gow, A.J., Corley, J., Pattie, A., 2015. Coupled changes in brain white matter microstructure and fluid intelligence in later life. J. Neurosci. 35, 8672–8682.
Rypma, B., Prabhakaran, V., Desmond, J.E., Glover, G.H., Gabrieli, J.D., 1999. Load-dependent roles of frontal brain regions in the maintenance of working memory. Neuroimage 9, 216–226.
Rypma, B., D'Esposito, M., 2000. Isolating the neural mechanisms of age-related changes in human working memory. Nat. Neurosci. 3, 509–515.
Salminen, L.E., Conturo, T.E., Laidlaw, D.H., Cabeen, R.P., Akbudak, E., Lane, E.M., Heaps, J.M., Bolzenius, J.D., Baker, L.M., Cooley, S., 2016. Regional age differences in gray matter diffusivity among healthy older adults. Brain Imag. Behav. 10, 203–211.
Salthouse, T.A., 2004. What and when of cognitive aging. Curr. Direct. Psychol. Sci. 13, 140–144.
Sexton, C.E., Walhovd, K.B., Storsve, A.B., Tamnes, C.K., Westlye, L.T., Johansen-Berg, H., Fjell, A.M., 2014. Accelerated changes in white matter microstructure during aging: A longitudinal diffusion tensor imaging study. J. Neurosci. 34, 15425–15436.
Shahab, S., Mulsant, B.H., Levesque, M.L., Calarco, N., Nazeri, A., Wheeler, A.L., Foussias, G., Rajji, T.K., Voineskos, A.N., 2019. Brain structure, cognition, and brain age in schizophrenia, bipolar disorder, and healthy controls. Neuropsychopharmacology. 44, 898–906.
Sowell, E.R., Peterson, B.S., Thompson, P.M., Welcome, S.E., Henkenius, A.L., Toga, A. W., 2003. Mapping cortical change across the human life span. Nat. Neurosci. 6, 309–315.
Stamatakis, E.A., Shafto, M.A., Williams, G., Tam, P., Tyler, L.K., 2011. White matter changes and word finding failures with increasing age. PLoS One 6.
Tau, G.Z., Peterson, B.S., 2010. Normal development of brain circuits. Neuropsychopharmacology. 35, 147–168.
Tibshirani, R., 1996. Regression Shrinkage and Selection Via the Lasso. J. Roy. Stat. Soc.: Ser. B (Methodol.) 58, 267–288.
Tulsky, D.S., Ivnik, R., Price, L.R., Wilkins, C., 2003. Assessment of cognitive functioning with the WAIS-III and WMS-III: Development of a six-factor model. Clin. Interpretation WAIS-III and WMS-III. 147–179.
Venkatesh, A., Stark, S.M., Stark, C.E.L., Bennett, I.J., 2020. Age- and memory- related differences in hippocampal gray matter integrity are better captured by NODDI compared to single-tensor diffusion imaging. Neurobiol. Aging 96, 12–21.
Viña, J., Borrás, C., Miquel, J., 2007. Theories of ageing. IUBMB Life 59, 249–254.
Wechsler, D., 1999. Wechsler abbreviated scale of intelligence. Vol., Psychological Corporation.
Westlye, L.T., Walhovd, K.B., Dale, A.M., Bjørnerud, A., Due-Tønnessen, P., Engvig, A., Grydeland, H., Tamnes, C.K., Østby, Y., Fjell, A.M., 2010. Life-span changes of the human brain white matter: diffusion tensor imaging (DTI) and volumetry. Cereb. Cortex 20, 2055–2068.
Wickett, J.C., Vernon, P.A., Lee, D.H., 2000. Relationships between factors of intelligence and brain volume. Personality Individ. Differ. 29, 1095–1122.
Yamada, H., Abe, O., Shizukuishi, T., Kikuta, J., Shinozaki, T., Dezawa, K., Nagano, A., Matsuda, M., Haradome, H., Imamura, Y., 2014. Efficacy of distortion correction on diffusion imaging: comparison of FSL eddy and eddy_correct using 30 and 60 directions diffusion encoding. PLoS One 9, e112411.